

Effectiveness of fibers and binders in high-strength concrete under chemical corrosion

Mahdi Nematzadeh* and Saber Fallah-Valukolaee^a

Department of Civil Engineering, University of Mazandaran, Babolsar, Iran

(Received June 6, 2017, Revised September 4, 2017, Accepted September 6, 2017)

Abstract. Investigating the properties and durability of high-strength concrete exposed to sulfuric acid attack for the purpose of its application in structures exposed to this acid is of utmost importance. In this research, the resistance and durability of high-strength concrete containing macro-polymeric or steel fibers together with the pozzolans of silica fume or nano-silica against sulfuric acid attack are explored. To accomplish this goal, in total, 108 high-strength concrete specimens were made with 9 different mix designs containing macro-polymeric and steel fibers at the volume fractions of 0.5, 0.75, and 1.0%, as well as the pozzolans of silica fume and nano-silica with the replacement levels of 10 and 2%, respectively. After placing the specimens inside a 5% sulfuric acid solution in the periods of 7, 21, and 63 days of immersion, the effect of adding the fibers and pozzolans on the compressive properties, ultrasonic pulse velocity (UPV), and weight loss of high-strength concrete was investigated and the respective results were compared with those of the reference specimens. The obtained results suggest the dependency of the resistance and durability loss of high-strength concrete against sulfuric acid attack to the properties of fibers as well as their fraction in concrete volume. Moreover, compared with using nano-silica, using silica fume in the fibrous concrete mix leads to more durable specimens against sulfuric acid attack. Finally, an optimum solution for the design parameters where the crushing load of high-strength fibrous concrete is maximized was found using response surface method (RSM).

Keywords: sulfuric acid attack; fibers; silica fume; nano-silica; ultrasonic test; crushing load; high-strength concrete; response surface method; optimization

1. Introduction

In recent decades, the effect of many environmental factors such as acid attack on concrete durability has taken into account in the design of structures, and in particular infrastructures. Generally, one of the main discussion regarding the durability of concrete structures is concrete exposure to acid environments, which affect the performance, lifetime, and maintenance cost of vital structural infrastructures. In fact, previous research has shown that the acids solved in ground water and chemical waste water, as well as those produced by oxidation of sulfur compounds in backfill can attack concrete substructure members and affect their durability (Fattuhi and Hughes 1988, Hobbs and Taylor 2000). Furthermore, the deterioration of sewage pipes and wastewater purification structures under sulfuric acid attack is considered as a global challenge that leads to grave problems such as reduced transfer capacity of sewage systems, pollution of soil and ground water, and ground settlement (Chang *et al.* 2005).

The degree of acid attack influence depends on their concentration and concrete permeability. If concrete is too permeable, acidic water can easily penetrate and increase its porosity through excessive washing of calcium hydroxide,

such that concrete becomes increasingly weaker and more susceptible to chemical attack. Hence, the demand for employing high-strength concrete (HSC) as a more compact concrete type with less permeability relative to conventional concrete has increased (Nematzadeh and Hasan-Nattaj 2017, Afroughsabet and Ozbakkaloglu 2015, Shannag 2000). On the other hand, since the use of these concrete types in structures has increased, their corresponding structural behavior has become more brittle accordingly. In this regard, evidence has shown that the brittle nature of HSC can be eliminated via the addition of fibers to the concrete mix (Hsu and Hsu 1994, Hasan-Nattaj and Nematzadeh 2017). Due to improving the ductility and enhancing the physico-mechanical properties of concrete, fibers are widely used (Zarrin and Khoshnoud 2016, Fallah and Nematzadeh 2017, Aslani and Natoori 2013). Furthermore, one common way used to improve concrete behavior against corrosion and acid attack is to add fibers to concrete volume (Mangat and Gurusamy 1988, Miao *et al.* 2002). By bridging cracks, fibers prevent the propagation and growth of micro- and macro-cracks, thus preventing acid penetration into concrete. However, the steel fibers in the vicinity of concrete cover are always at risk of corrosion; hence, depending on the degree of fiber corrosion, concrete properties are negatively affected (Hwang *et al.* 2015). Therefore, synthetic fibers such as macro-polymeric fibers can be used to resist against acid attack, which were employed and investigated in the current study. Other methods applied to limit damage caused by acid attack include the use of supplementary cementitious

*Corresponding author, Assistant Professor

E-mail: m.nematzadeh@umz.ac.ir

^aGraduate Student

materials such as fly ash, silica fume, and nano-silica in concrete mix to improve resistance against sulfuric acid attack through reducing the content of calcium hydroxide present in the concrete mix, which is more vulnerable to acid attack (Mehta 1985, Torii and Kawamura 1994, Tamimi 1997). The effect of pozzolans on enhancing concrete durability in acid environments is attributed to the improvement of pore structures (due to fine pozzolan particles), the reduction of permeability, as well as the reduction in the amount of calcium hydroxide together with the increase in the amount of calcium silicate hydrate (C-S-H) gel produced by pozzolanic reaction (Mehta 1985). In fact, while attacking concrete, sulfuric acid reacts with the calcium hydroxide present in the concrete and produced by hydration reaction, which results in the formation of gypsum ($\text{CaSO}_4 \cdot 2\text{H}_2\text{O}$). Although gypsum formation is accompanied by the volumetric expansion of about twice as much, some researchers have suggested that this reaction plays a secondary role in the erosion process of concrete. In this regard, the reaction between gypsum and tricalcium aluminate (C_3A) in the presence of water produces voluminous ettringite ($\text{C}_6\text{AS}_3\text{H}_{32}$). The corresponding volumetric expansion (nearly 7 times) produces inner pressure in the concrete pores, resulting in its expansion, which in turn leads to the formation of cracks in concrete and the subsequent deterioration of erosion condition (Monteny *et al.* 2000, Monteny *et al.* 2001). As the concrete erosion proceeds, the cracked surface acquires a soft and whitish appearance, and thus the corroded concrete loses its mechanical strength and durability, as a consequence of further cracking and spalling, which ultimately leads to its total destruction (Lee *et al.* 2008, Santhanam *et al.* 2002, Schmidt *et al.* 2009).

Different studies have so far been performed on the effect of cement type, water/cement ratio (Fattuhi and Hughes 1988, Ehrich *et al.* 1999, Suleiman *et al.* 2014), supplementary cementitious materials (Mehta 1985, Torii and Kawamura 1994, Tamimi 1997), recycled aggregates as natural aggregate replacement in concrete, and aggregate type (Chang *et al.* 2005, Rahimi *et al.* 2016, Araghi *et al.* 2015) to enhance the behavior of conventional concrete under acid attack. Today, fibrous concrete is being increasingly employed on a global scale due to presenting better mechanical properties and durability. Therefore, employing this concrete type in construction industry requires more research into its properties and durability, which are of particular interest in the design and construction of infrastructures and special structures.

This current study is an experimental investigation of the compressive behavior of high-strength concrete containing different percentages of macro-polymeric or steel fibers in the presence of the pozzolans of silica fume or nano-silica under sulfuric acid attack. Since adding fibers to concrete mix may alter erosion development mechanisms in concrete, the effect of different fiber contents on the performance of concrete under sulfuric acid attack was explored. Both macro-polymeric and steel fibers were used in three different volume fractions, i.e., 0.5, 0.75, and 1.0%, and silica fume and nano-silica were used in the concrete mix with the replacement levels of 10 and 2%, respectively,

Table 1 Chemical composition and physical properties of cementitious materials

Item	Cementitious materials (%)		
	Cement	Nano-silica	Silica fume
SiO_2	21.75	≥ 98	93
Al_2O_3	5.1	0.076	1.7
Fe_2O_3	4.0	0.293	1.2
CaO	64.0	0.392	0.3
MgO	1.85	0.05	1
SO_3	2.0	0.185	-
Na_2O	0.55	0.328	0.6
K_2O	0.55	0.080	1.1
TiO_2	-	0.064	-
P_2O_5	-	0.129	-
ZnO	-	0.021	-
CuO	-	0.020	-
Loss on ignition	1.5	-	0.4 - 3
Insoluble Residue	0.35	-	-
Free CaO	0.7	-	-
Compounds			
C_3S	55.0	-	-
C_2S	20.0	-	-
C_3A	6.5	-	-
C_4AF	11	-	-
Physical properties			
Specific gravity	3.15	2.65	2.21
Specific surface (m^2/gr)	0.305	193	14

by the cement weight. After immersing the concrete specimens in a 5% sulfuric acid solution for the periods of 7, 21, and 63 days immersion, the changes in the physico-mechanical properties of the concrete specimens including ultrasonic pulse velocity (UPV), crushing load, weight, and appearance were investigated. At last, an optimum solution for the design parameters, for which the crushing load of fibrous concrete is maximized, was obtained using the response surface method (RSM).

2. Experimental program

2.1 Materials

Here, type II Portland cement with the specific gravity of 3.15, as well as silica fume and nano-silica with the replacement levels of 10 and 2%, respectively, by the cement weight were used in concrete mix. Table 1 lists the chemical composition and physical properties of cement, silica fume, and nano-silica (provided by manufacturer). Coarse aggregate with the specific gravity of 2.69, water absorption of 0.47%, and the maximum nominal size of 12.5 mm, and fine aggregate with the fineness modulus of 2.6, specific gravity of 2.63, water absorption of 1.73%, and the maximum nominal size of 4.75 mm were used.

In this study, macro-polymeric fibers with the length and aspect ratio (l/d) of 39 mm and 50, respectively, were

Table 2 Physical and mechanical properties of fibers

Type of fiber	Shape of fiber	Length l (mm)	Diameter d (mm)	Aspect ratio l/d	Density (kg/m ³)	Tensile strength (MPa)	Elastic modulus (GPa)
Macro-polymeric (MP)	Crimped	39	0.78	50	910	500	3.6
Steel (ST)	Hooked-end	50	0.8	62.5	7850	1400	200



(a) Macro-polymeric fibers



(b) Steel fibers

Fig. 1 Shape and dimension of different types of fibers

employed in three different volume fractions, i.e., 0.5, 0.75, and 1.0%, and hooked-end steel fibers with the length and aspect ratio of 50 mm and 62.5, respectively, were used in the same volume fractions of 0.5, 0.75, and 1.0%. The physical and mechanical properties of the fibers used in this study are presented in Table 2. In addition, Fig. 1 shows photos of the fibers used. A superplasticizer based on polycarboxylate ether commercially available under the name of SPC10 with the solid content of 42% was used in all the concrete mixes as a weight percentage of total cementitious materials.

2.2 Specimens

Here, the total of 108 cubic 100×100×100 mm specimens were made in 9 groups composed of 12 specimens to investigate the effect of different contents of macro-polymeric and steel fibers on the variations of the parameters of weight, UPV, and crushing load of the high-strength concrete specimens containing silica fume and nano-silica at the ages of 0, 7, 21, and 63 days immersion in the sulfuric acid solution. To reduce error, three identical specimens were prepared, and their results were averaged and reported as the final result.

The specimens in this work were named in terms of test variables, and a guide to identify the specimens based on their given names, is provided in Fig. 2. According to the figure, MP and ST indicate the presence of macro-polymeric and steel fibers, respectively, in the concrete mix, with the following number giving the volume fraction of

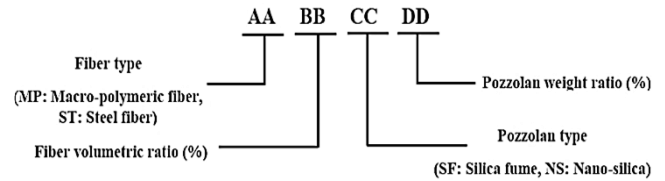


Fig. 2 Labeling specimens in terms of test variables

fibers used. Furthermore, NS and SF represent the inclusion of nano-silica and silica fume, respectively, in the concrete mix, and the following number is the weight percentage of the cement-replacing pozzolan.

2.3 Mix design and sample preparation

The concrete mix proportions in one cubic meter according to the ACI 211.4R specifications (2008) are presented in Table 3. In this research, as can be seen in the table, 9 series of mix designs with the same water/cementitious materials ratio equal to 0.31 were made, including one concrete mix containing silica fume and without fibers, six fibrous concrete mixes containing silica fume, and two fibrous concrete mixes containing nano-silica.

To prepare the concrete mix, first the aggregates including gravel and sand were mixed in a mixer for 30 sec, then cement was combined with the pozzolan of interest, and the result was added to the aggregate mix to be stirred for another 1 min. In the next step, a mixture of water and the superplasticizer, which also included the water needed to raise the aggregate moisture to the saturated surface dry condition, was poured gently into the mixer for 30 sec, and the resulting mixture was stirred for 2 min. Finally, in the case of fiber inclusion in the mix design, the stirring continued for 2 more minutes in the mixer. After the end of mixing procedure, in order to determine the workability of the fresh concrete, the slump of the concrete mixes was measured in accordance with ASTM C143 (2015); the obtained values are listed in Table 3. The fresh concrete was cast into 100×100×100 mm cubic molds in two layers, each tamped 25 times with a tamping rod. Once the fresh concrete was cast into the molds, a vibrating table was employed to further compact the concrete and reduce the number of entrapped air bubbles. After 24 hours, the specimens were unmolded and cured for at least 28 days at the standard temperature of 23°C and relative humidity of 100%. Fig. 3 shows photos of the fresh and hardened concretes.

2.4 Test methods

Following the curing procedure, the specimens were transferred into a 5% sulfuric acid solution (pH=1). Fig.

Table 3 Mix proportions of high-strength concrete mixes

Mix No.	Mixture ID	W/B	Water	Cement	Silica fume	Nano silica	Fine Aggregates	Coarse Aggregates	Fiber type	Fiber V_f (%)	SP (%)*	Slump (mm)
1	SF10 (Control)	0.31	161.2	468	52	-	805.2	914.3	-	-	0.7	150
2	MP0.5SF10	0.31	161.2	468	52	-	805.2	914.3	MP	0.5	0.7	150
3	MP0.75SF10	0.31	161.2	468	52	-	805.2	914.3	MP	0.75	0.7	150
4	MP1.0SF10	0.31	161.2	468	52	-	805.2	914.3	MP	1.0	0.7	150
5	ST0.5SF10	0.31	161.2	468	52	-	805.9	914.3	ST	0.5	0.9	125
6	ST0.75SF10	0.31	161.2	468	52	-	806.2	914.3	ST	0.75	1.0	113
7	ST1.0SF10	0.31	161.2	468	52	-	806.5	914.3	ST	1.0	1.1	100
8	MP0.75NS2	0.31	161.2	509.6	-	10.4	806.8	914.3	MP	0.75	1.2	140
9	ST0.75NS2	0.31	161.2	509.6	-	10.4	807.1	914.3	ST	0.75	1.3	80

*Percentage of total weight of cementitious materials

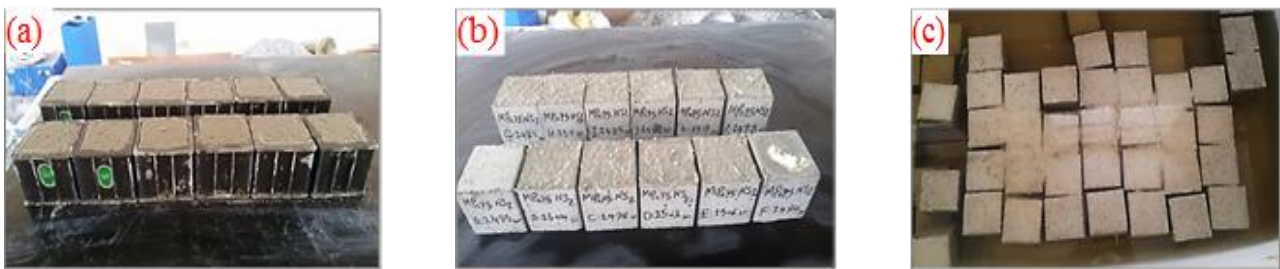


Fig. 3 A view of (a) fresh concrete specimens; (b) hardened concrete specimens; (c) specimens immersed in 5% sulfuric acid solution

3(c) shows the concrete specimens immersed in a 5% sulfuric acid solution. In order to keep the solution pH fixed, the amount of sulfuric acid required to do so was added to the original acid solution on a weekly basis such that the acid concentration of the solution would not change. After extraction, the specimens immersed in the acid tank were rinsed with tap water three times to remove loose reaction products. After the specimens were dried at ambient temperature for 30 min, their dimensions and weight were measured, followed by UPV and compressive testing. Additionally, weight loss percentage at any given time was measured as an indicator of concrete deterioration under sulfuric acid attack. Furthermore, the reduction in the UPV and load-bearing capacity values relative to the reference values (the experimental results of specimens after 28 days of curing without being exposed to acid) was determined. While measuring the compressive strength of the acid-exposed specimens, several difficulties appear regarding the measurement of the specimen dimensions after acid exposure, since the specimen dimensions become irregular after the exposure of aggregates to acid. As a result, the load-bearing capacity of a cubic specimen may be determined based on the maximum load recorded in a compressive test. This compressive load in the test specimens before and after acid attack is known as the crushing load and its measurement method as the crushing load test (Chang *et al.* 2005).

In order to measure the ultrasonic pulse velocity in compliance with ASTM C597 (2016), an ultrasonic nondestructive electronic device with the precision of 0.1 μ s was employed. The nondestructive testing of the specimens

was performed at specified exposure ages in order to determine the ultrasonic pulse transmission time through the direct transmission method and by using the Pundit tester device (Model PC 1012). A transducer with the vibration frequency of 54 kHz and the accuracy of $\pm 1\%$ for travel time and $\pm 2\%$ for distance was also utilized. In all the tests, refractory grease was used to connect the transducers to the flat, smooth concrete surface. For each test on the concrete specimens, five readings were performed by switching the position of the transducers on the two opposite faces, and the reported final result was the mean value of the five readings.

After determining the experimental results of transmission time, the ultrasonic pulse velocity in the concrete specimens was calculated as the ratio of the transmission distance (the distance between the measurement faces) to the transmission time. Following the nondestructive testing on the concrete specimens, the compressive testing was also performed on the cubic specimens with the loading rate of 0.25 MPa/s being in the allowed range specified by the BS 1881-116 (1983) (0.2-0.4 MPa/s), and then, the crushing load values of all the specimens were determined in kN. Furthermore, for the purpose of visual inspection and documenting the changes in surface appearance, the cubic specimens were photographed after the end of immersion period and removal from the acid solution.

3. Test results and discussion

Table 4 Crushing load test results

Mix No.	Mixture ID	Crushing load (kN)							
		Immersion in 5% sulfuric acid solution							
		0 day *	COV (%)	7 days	COV (%)	21 days	COV (%)	63 days	COV (%)
1	SF10 (Control)	695.0	6.5	562.0	1.8	510.0	1.9	491.7	8.9
2	MP0.5SF10	743.5	1.4	563.3	6.7	544.0	9.0	522.3	4.7
3	MP0.75SF10	720.5	2.5	593.7	5.2	591.7	7.5	570.3	9.3
4	MP1.0SF10	638.7	2.6	535.0	4.9	495.3	5.6	420.0	7.0
5	ST0.5SF10	807.0	5.4	747.0	4.9	749.3	3.3	706.3	6.7
6	ST0.75SF10	835.7	5.5	749.0	4.9	679.0	9.5	634.0	9.9
7	ST1.0SF10	866.0	1.3	707.0	7.6	626.7	5.0	615.3	3.7
8	MP0.75NS2	646.0	5.0	528.3	1.3	470.0	5.2	459.0	6.5
9	ST0.75NS2	646.5	6.0	564.0	7.8	516.0	6.9	386.0	9.7

*After at least 28 days of curing without acid exposure

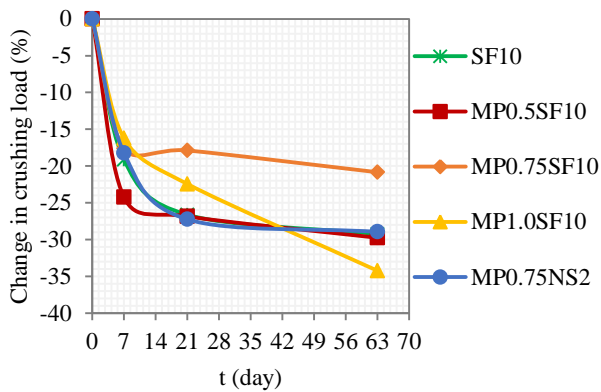


Fig. 4 Relative variations of crushing load for concrete specimens containing macro-polymeric fibers after immersion in 5% sulfuric acid solution

3.1 Crushing load

Little research has been conducted to compare the effectiveness of synthetic and steel fibers, among which the one performed by Kim *et al.* (2015) focused on the compressive strength and durability of concrete reinforced with different fibers and exposed to a solution with pH=4.5. Their results showed that the concrete reinforced with steel fibers had superior performance relative to that of the concretes reinforced with PP and PVA fibers in terms of durability and strength.

The crushing load results of the specimens after 7, 21, and 63 days immersion in the sulfuric acid solution together with the corresponding results of the reference specimens (after at least 28 days of curing without acid exposure) are given in Table 4. The variations of the crushing load of the concrete specimens reinforced with macro-polymeric fibers and immersed in the acid solution relative to the reference values versus immersion time are shown in Fig. 4. As can be seen in the figure, the reduction trend of crushing load in all the specimens begins at early immersion ages, and the intensity of load-bearing capacity reduction is higher in these early days, with the highest reduction for the specimen containing 0.5% macro-polymeric fibers and 10%

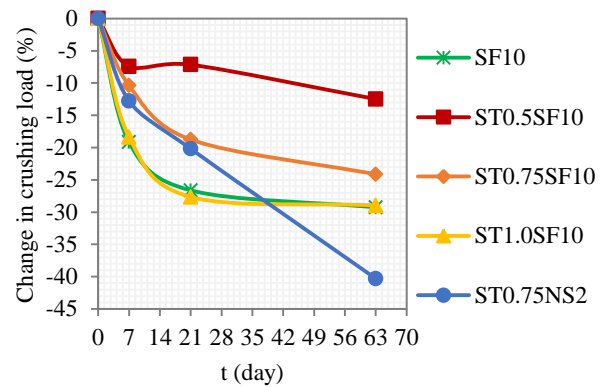


Fig. 5 Relative variations of crushing load for concrete specimens containing steel fibers after immersion in 5% sulfuric acid solution

silica fume. Moreover, after 7 days immersion in the acid solution, the crushing load reduction rate of the specimens demonstrates a significant decrease; however, further adding macro-polymeric fibers more than 0.75% in the concrete containing 10% silica fume preserves the reducing trend of crushing load up to 63 days immersion due to the high fiber volume fraction used; the fact that is the consequence of fiber agglomeration and subsequent pore formation in fibrous concrete. At high immersion ages, the specimens containing 0.75% macro-polymeric and 10% silica fume have the lowest resistance reduction. Crushing load reduction after 63 days immersion in sulfuric acid for the fiber-lacking concrete specimen and those containing 0.5, 0.75, and 1.0% macro-polymeric fibers relative to that of the corresponding reference specimens is 29.3, 29.7, 20.8, and 34.2%, respectively.

It is also found from Fig. 4 that using 2% nano-silica in comparison with using 10% silica fume as a cement replacement in the specimen reinforced with 0.75% macro-polymeric fibers leads to a greater reduction trend in the crushing load during the immersion period; the reduction in crushing load after 63 days immersion in sulfuric acid for the specimen containing 0.75% macro-polymeric and 2% nano-silica (MP0.75NS2) is 28.9% relative to the corresponding reference specimen. Therefore, it can be concluded that the specimen MP0.75SF10 demonstrated better resistance against sulfuric acid attack. In addition, it can be understood from the figure that the crushing load reduction values of the specimens MP0.75NS2 and SF10 during the immersion period are almost similar to each other, with a negligible reduction rate after 21 days immersion.

The variations of the crushing load of the concrete specimens reinforced with steel fibers and immersed in the acid solution relative to the corresponding reference values versus the immersion time are shown in Fig. 5. As can be seen, as the volume fraction of steel fibers in the concrete containing 10% silica fume increases, so does the crushing load reduction trend up to 63 days immersion, which is attributed to fiber agglomeration and pore formation in the fibrous concrete. Hence, it is found that the specimen containing 0.5% steel fibers showed a proper resistance

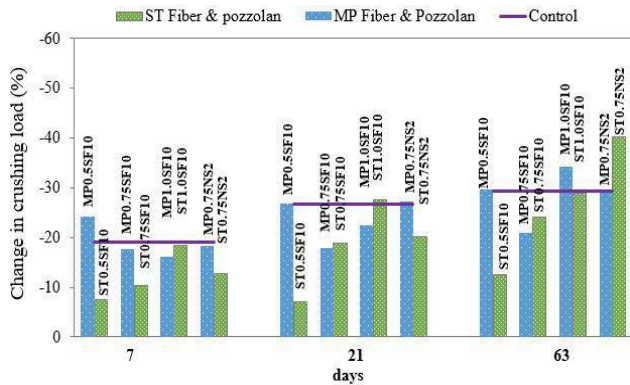


Fig. 6 Comparison between the crushing load variations of concrete specimens containing steel fibers and those containing macro-polymeric fibers versus immersion time in acid solution

against sulfuric acid ions. However, the rate of resistance loss after 21 days immersion experiences a significant reduction in all the fibrous concrete specimens containing silica fume. The crushing load reduction after 63 days immersion in sulfuric acid for the fiber-lacking specimen and those containing 0.5, 0.75, and 1.0% steel fibers relative to that of the corresponding reference specimens is 29.3, 12.5, 24.1, and 28.9%, respectively.

It is also found from Fig. 5 that using 10% silica fume in relation to 2% nano-silica as a cement replacement in the specimen containing 0.75% steel fibers results in the improvement of the crushing load reduction trend versus immersion time. Moreover, the specimen containing nano-silica shows a similar resistance reduction trend to that of the corresponding specimen containing silica fume up to 21 days immersion in the acid solution, and above which, the resistance loss rate in the concrete containing silica fume undergoes a considerable decrease in contrast to the nano-silica-containing specimen. The reduction in crushing load after 63 days immersion in sulfuric acid for the specimen containing 0.75% steel fibers and 2% nano-silica relative to that of the corresponding reference specimen is 40.3%. In addition, it is also observed in the figure that the fiber-lacking concrete specimen and the one containing 1.0%

steel fibers have nearly similar decreasing trend up to 63 days immersion and show greater resistance reduction compared with the other silica fume-containing specimens. The variations of the crushing load of the concrete specimens reinforced with steel fibers relative to that of the specimens containing macro-polymeric fibers versus the immersion time in the sulfuric acid solution are shown in Fig. 6, where the concrete containing silica fume and without fibers is considered as the control concrete. It is observed in the fiber-reinforced concrete specimens containing silica fume that the specimen containing 0.5% steel fibers demonstrates considerably lower crushing load variations relative to those of the specimen containing 0.5% macro-polymeric fibers during the immersion time of up to 63 days. Furthermore, in the other specimens containing higher fiber volume fractions, the difference between the results of the concretes containing steel fibers and those with macro-polymeric fibers decreases; a fact that implies the more effective bridging action of high fiber volume fractions against the cracks induced by the inner pressures resulted from the volumetric expansion of cement paste during the reaction with sulfuric acid. Moreover, in the fibrous specimens containing silica fume, the response difference between the concretes containing steel fibers and those with macro-polymeric fibers relatively decreases in high immersion days.

It can also be seen in Fig. 6 that in the fibrous concrete specimens containing nano-silica, the crushing load variations of the specimen containing steel fibers demonstrate greater reduction trend in comparison with those of the specimen containing macro-polymeric fibers after 21 days immersion, which can be attributed to good bond between macro-polymeric fibers and the nano-silica-containing concrete matrix. Furthermore, the concrete specimen containing nano-silica and steel fibers (ST0.75NS2) has the highest resistance loss at the immersion age of 63 days among all the specimens.

3.2 Ultrasonic pulse velocity

The UPV test results of the specimens after 7, 21, and 63 days immersion in the sulfuric acid solution together

Table 5 Experimental results of ultrasonic pulse velocity and weight

Mix No.	Mixture ID	Immersion in 5% sulfuric acid solution							
		Ultrasonic pulse velocity (km/s)				Weight (kg)			
		0 day*	7 days	21 days	63 days	0 day*	7 days	21 days	63 days
1	SF10 (Control)	5.22	4.85	4.71	4.66	2.483	2.412	2.403	2.376
2	MP0.5SF10	5.25	4.85	4.81	4.75	2.463	2.392	2.349	2.313
3	MP0.75SF10	5.23	4.88	4.86	4.82	2.485	2.408	2.392	2.356
4	MP1.0SF10	5.19	4.80	4.69	4.42	2.468	2.396	2.361	2.312
5	ST0.5SF10	5.33	5.27	5.27	5.22	2.542	2.499	2.483	2.476
6	ST0.75SF10	5.36	5.27	5.21	5.08	2.570	2.498	2.473	2.468
7	ST1.0SF10	5.42	5.22	5.02	4.95	2.575	2.466	2.414	2.392
8	MP0.75NS2	5.15	4.78	4.60	4.48	2.513	2.408	2.341	2.333
9	ST0.75NS2	5.16	4.86	4.71	4.34	2.580	2.466	2.412	2.398

*After at least 28 days of curing without acid exposure

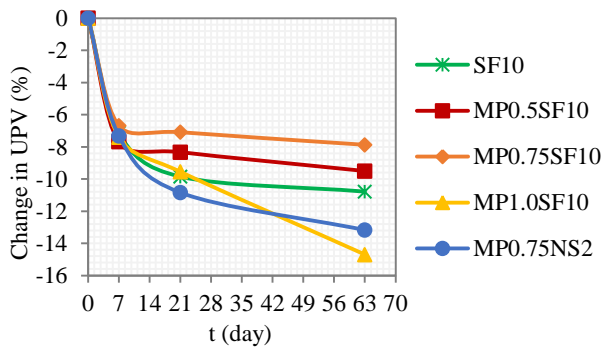


Fig. 7 Relative variations of UPV of concrete specimens containing macro-polymeric fibers after immersion in 5% sulfuric acid solution

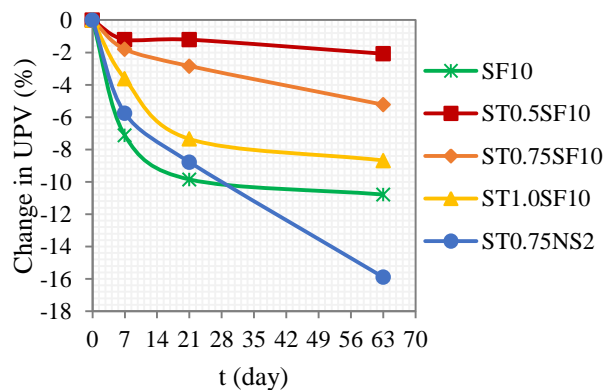


Fig. 8 Relative variations of UPV of concrete specimens containing steel fibers after immersion in 5% sulfuric acid solution

with the results of the reference specimens are listed in Table 5. The coefficient of variation (COV) obtained from the results of the specimens on UPV and weight is not considered here due to the closeness of the results and the consistency of the specimens.

Fig. 7 shows the variations of the UPV of the specimens containing macro-polymeric fibers immersed in acid in relation to the reference values versus immersion time. As can be seen in the figure, the reduction trend of UPV is almost the same for all the specimens up to 7 days of immersion. Furthermore, adding macro-polymeric fibers up to the volume fraction of 0.75% in the concrete containing silica fume decreases the UPV loss up to 63 days immersion; however, as the volume fraction of macro-polymeric fibers increases above that threshold (volume fraction of 1.0%), the loss of UPV during the immersion time experiences a significant increase, due to pores formed as a result of fiber agglomeration. The UPV reduction after 63 days immersion in sulfuric acid for the concrete specimen without fibers and those containing 0.5, 0.75, and 1.0% macro-polymeric fibers relative to that of the corresponding reference specimens is 10.8, 9.5, 7.9, and 14.7%, respectively.

Fig. 7 also shows that using 2% nano-silica compared with 10% silica fume as a cement-replacement in the specimen containing 0.75% macro-polymeric fibers leads to

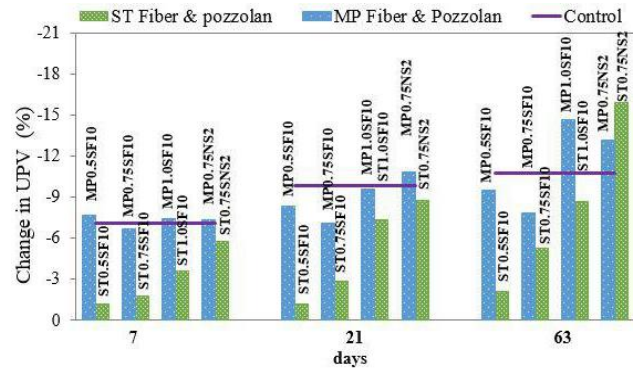


Fig. 9 Comparison between the UPV variations of concrete specimens containing steel fibers and those containing macro-polymeric fibers versus immersion time in acid solution

a greater reducing trend of the UPV during immersion time; however, the behavior shown by each pozzolan is similar to that of the other up until 7 days immersion in acid solution. Reduction in the pulse velocity after 63 days immersion for the concrete containing 0.75% macro-polymeric fibers and 2% nano-silica relative to that of the corresponding reference concrete is 13.2%, while the concrete containing 0.75% macro-polymeric and 10% silica fume has the lowest value of UPV reduction due to acid attack.

Fig. 8 presents the variations of the UPV of the concrete specimens containing steel fibers and immersed in acid solution relative to the reference values versus immersion time. It shows that the addition of steel fibers in the concrete containing silica fume leads to a decrease in the UPV reduction in comparison with the fiber-lacking specimen (SF10) up to 63 days immersion in the acid solution, with the specimen containing 0.5% steel fibers exhibiting the best performance among all the specimens against sulfuric acid attack. The UPV reduction after 63 days immersion in the sulfuric acid solution relative to the UPV of the corresponding reference specimens for the fiber-lacking concrete specimen and those containing 0.5, 0.75, and 1.0% steel fibers is 10.8, 2.1, 5.2, and 8.7%, respectively. These results suggest that increasing the volume fraction of steel fibers leads to an increase in the reduction trend of UPV during immersion time in the acid solution; which is attributed to the formation of pores due to fiber agglomeration.

On the other hand, Fig. 8 shows that using 2% nano-silica in relation to 10% silica fume as a cement replacement in the specimen containing 0.75% steel fibers leads to a greater UPV reduction trend during immersion time, such that the UPV reduction of this specimen after 63 days immersion is significantly greater than that of the other specimens with the loss of 15.9% relative to the reference value.

Fig. 9 shows the UPV variations of the concrete specimens containing steel fibers relative to those containing macro-polymeric fibers versus immersion time in sulfuric acid solution. As can be seen in the figure, the UPV reduction of the concrete specimens containing steel fibers is clearly lower than that of the specimens containing

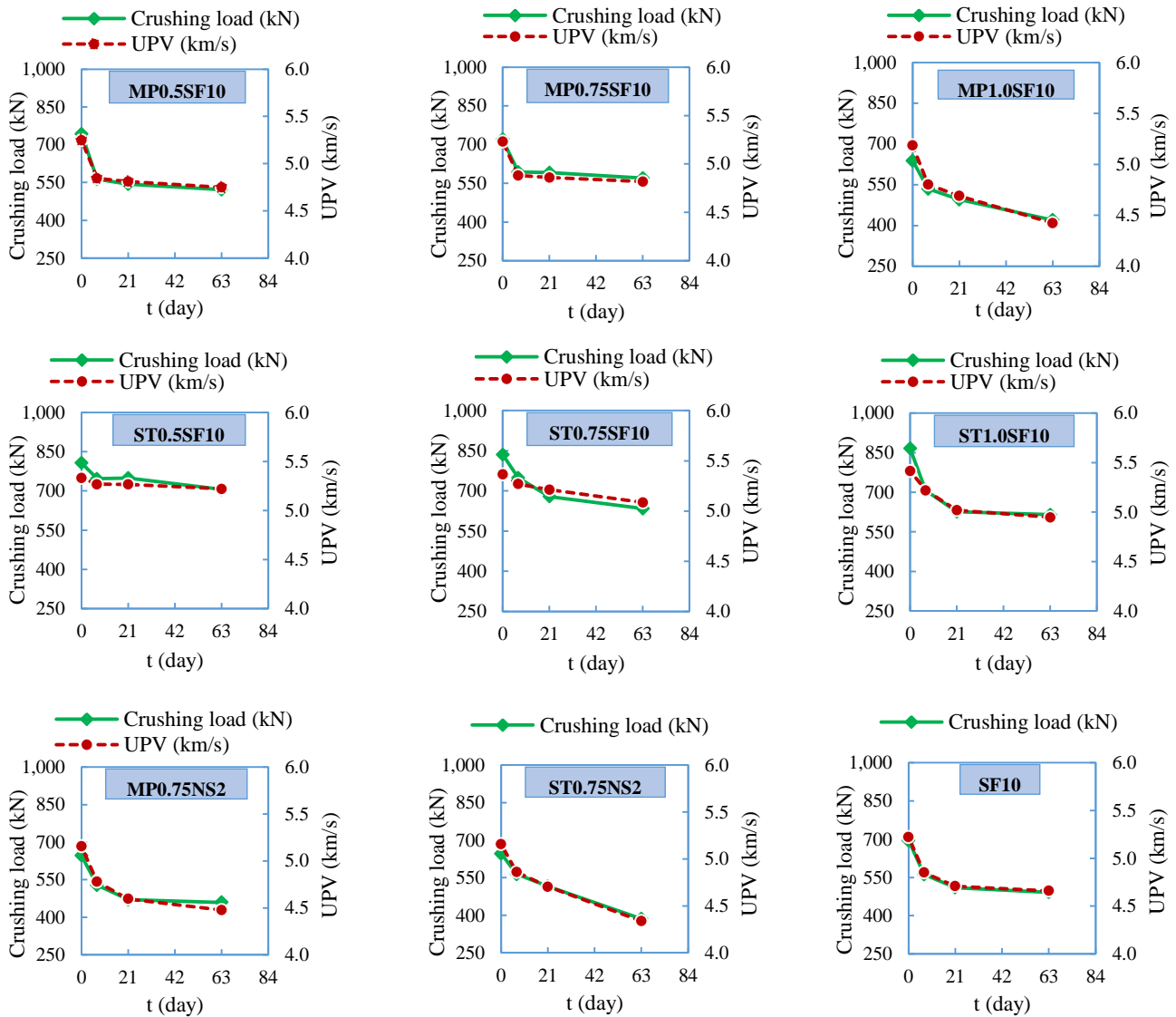


Fig. 10 Relationship between crushing load and UPV against immersion time in sulfuric acid solution

macro-polymeric fibers for all the fiber volume fractions and all the immersion periods; however, the UPV loss of the concrete mix reinforced with 0.75% macro-polymeric fibers and containing 2% nano-silica is lower than that of the concrete mix containing 0.75% steel fibers together with 2% nano-silica after 63 days immersion. In addition, the specimens containing steel fibers demonstrated lower UPV loss in comparison with the control (fiber-lacking) specimen. It is found from the results that the value of UPV loss after 63 days immersion for the specimens ST0.5SF10 and ST0.75NS2 represents the minimum and maximum UPV loss, respectively, among all the specimens.

Fig. 10 presents the relationship between the crushing load and UPV of the concrete specimens versus immersion time in the acid solution. Regarding the figure, the crushing load and UPV of the specimens demonstrate a rather identical decreasing trend against the immersion time; hence, by using the UPV method as a nondestructive test, the variations of the crushing load of the specimens with immersion time can be predicted properly. This fact may

indicate that with increasing immersion time and further penetration of acid into the concrete, the concrete specimen undergoes further destruction and erosion, resulting in a decreased crushing load. In addition, due to the higher porosity and lower integrity of concrete, the ultrasonic pulse velocity also experiences a reduction, similar to that of the crushing load.

Nevertheless, the percentage of UPV reduction is lower relative to the crushing load reduction, due to the presence of the sulfuric acid reaction products in the eroded (damaged) concrete.

The relationship between the crushing load and UPV of the specimens versus the volume fraction of macro-polymeric fibers at the immersion ages of 0, 7, 21, and 63 days in the sulfuric acid solution is shown in Fig. 11, from which it is understood that there is a good similarity between the variations of the crushing load and those of UPV against the volume fraction of macro-polymeric fibers. This suggests that a logical relationship exists between the values of these two parameters. With respect to the figure,

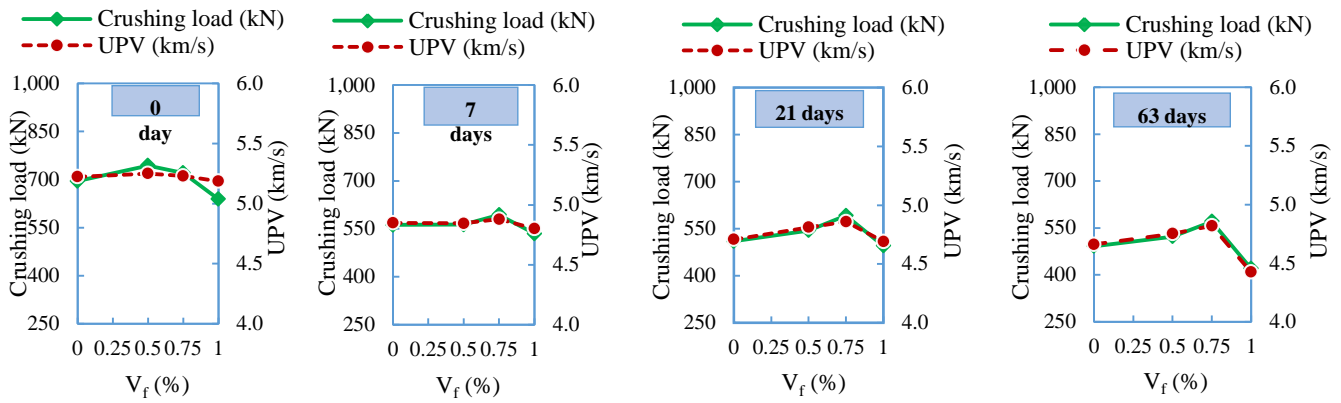


Fig. 11 Relationship between crushing load and UPV versus volume fraction of macro-polymeric fibers

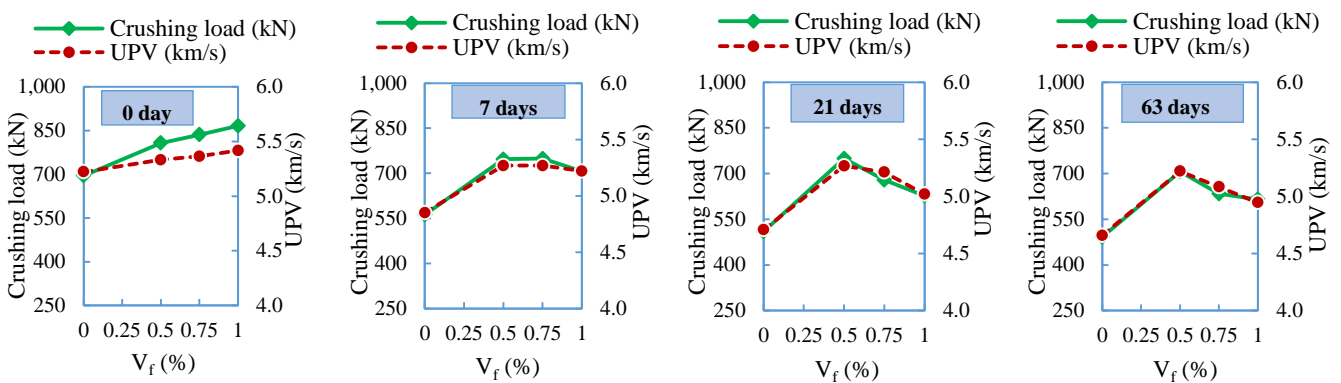


Fig. 12 Relationship between crushing load and UPV versus volume fraction of steel fibers

in specimens with the zero-day immersion in acid (reference specimens), as the volume fraction of macro-polymeric fibers increases up to 0.5%, the crushing load and UPV of the concrete also increases; however, as this volume fraction increases above that threshold, both the crushing load and UPV decreases, due to the pores induced by fiber agglomeration. A similar behavior is also observed after 7, 21, and 63 days immersion in acid solution, with the difference being the occurrence of the highest crushing load and UPV values of the specimens at the fiber volume fraction of 0.75%.

The relationship between the crushing load and UPV of the specimens versus the volume fraction of steel fibers at the immersion ages of 0, 7, 21, and 63 days in the sulfuric acid solution is shown in Fig. 12; according to which, there is a good similarity between the variations of the crushing load and those of UPV against the volume fraction of steel fibers. However, for the reference specimens, the curves do not completely coincide with each other, unlike what is observed for the specimens immersed in acid. Considering the figure, it is found that after 0 days immersion (reference specimens), as the volume fraction of steel fibers increases up to 1.0%, the crushing load and UPV of the concrete shows a significant increase in relation to those of the fiber-lacking concrete (SF10). However, after 7, 21, and 63 days to 0.5%, the crushing load and UPV show an increasing trend, and after that threshold, a decreasing trend is observed.

Generally, with respect to Figs. 11 and 12, it can be said that the concrete specimens containing steel fibers have higher sulfuric acid solution, thus the specimens containing steel immersion, with increasing volume fraction of steel fibers up fibers have higher crushing load and UPV.

3.3 Crushing load–Ultrasonic pulse velocity relationships

The UPV method is a nondestructive concrete test based on calculating the transmission velocity of ultrasonic pulses through concrete, and it is widely used to evaluate some of the mechanical properties and integrity of concrete structures (Solis-Carcaño and Moreno 2008, Bogas *et al.* 2013). Generally, by using UPV, properties such as the porosity, strength, and modulus of elasticity of concrete, as well as the depth of surface cracks, defects and the level of damage caused by chemical attack and fire can be explored (Hernández *et al.* 2000, Nwokoye and Eng 1974, Naffa *et al.* 2002, Trtnik *et al.* 2009).

Here, by employing nonlinear regression analysis of the experimental results, appropriate exponential functions for determining the crushing load-UPV relationship of the 9 groups of the specimens containing macro-polymeric or steel fibers are presented, as shown in Figs. 13 and 14, respectively. Regarding the figures, a very good relevance is observed between the data points and regression curves.

To present a general and applicable relationship between

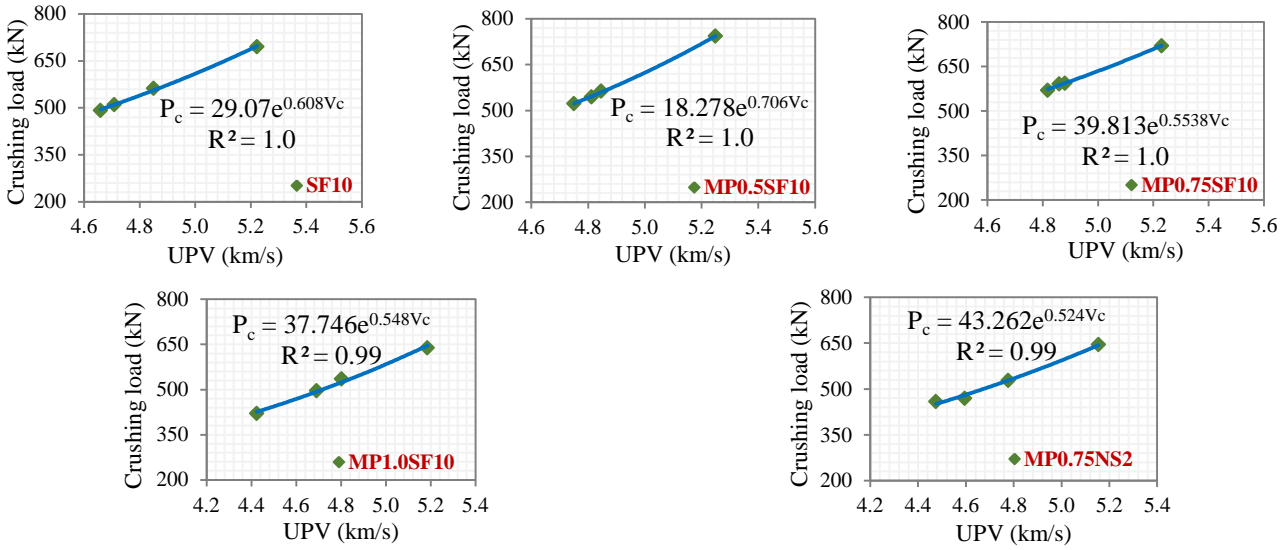


Fig. 13 Empirical relationships between crushing load and UPV together with experimental data for different groups containing macro-polymeric fibers

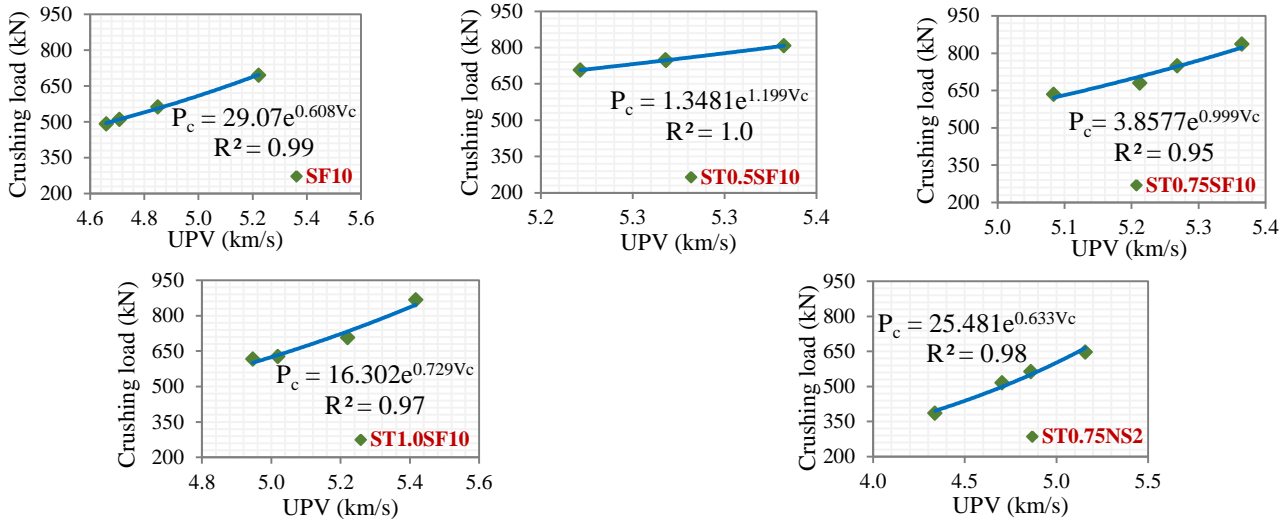


Fig. 14 Empirical relationships between crushing load and UPV together with experimental data for different groups containing steel fibers

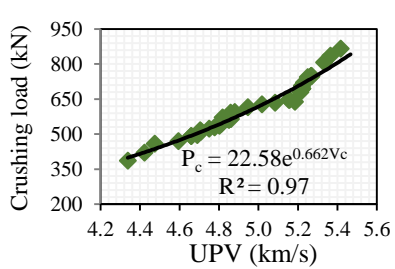


Fig. 15 Empirical relationship obtained between crushing load and UPV together with experimental data for all high-strength concrete specimens

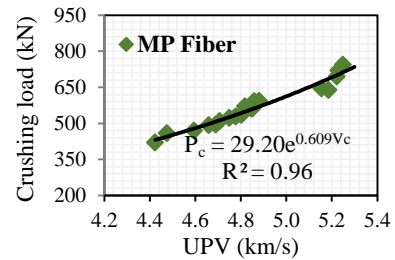


Fig. 16 Empirical relationship between crushing load and UPV together with experimental data for all specimens containing macro-polymeric fibers

crushing load and UPV, a nonlinear regression analysis of all the results obtained from the test specimens with various pozzolans and fibers at different volume fractions and at different immersion ages in acid was conducted, and the obtained result is presented as the following equation

having an appropriate coefficient of determination ($R^2=0.97$), as can be seen in Fig. 15.

$$P_c = 22.58e^{0.662V_c} \tag{1}$$

where P_c and V_c are the crushing load and UPV of the

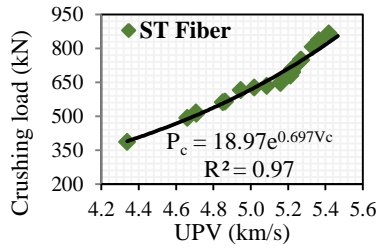


Fig. 17 Empirical relationship between crushing load and UPV together with experimental data for all specimens containing steel fibers

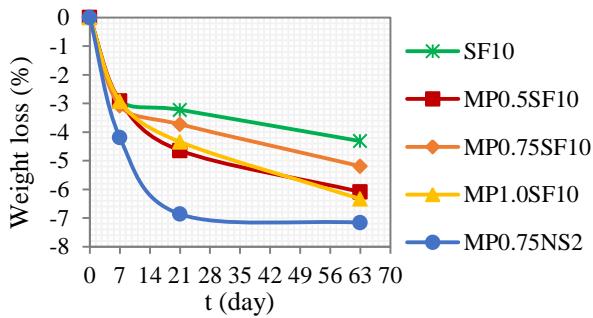


Fig. 18 Weight loss of specimens containing macro-polymeric fibers after exposure to a 5% sulfuric acid solution

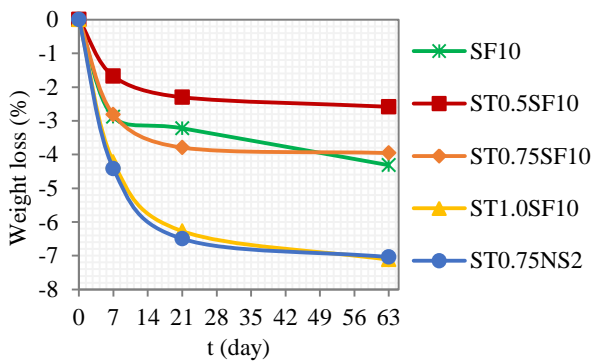


Fig. 19 Weight loss of specimens containing steel fibers after exposure to a 5% sulfuric acid solution

concrete specimens, respectively, expressed in terms of kN and km/s.

Furthermore, Figs. 16 and 17 show the empirical relationships obtained between P_c and V_c together with the experimental data of various high-strength concrete specimens containing macro-polymeric or steel fibers individually; the obtained relationships presented in the figures are expressed as Eqs. (2) and (3), respectively.

$$P_c = 29.20e^{0.609V_c} \quad (2)$$

$$P_c = 18.97e^{0.697V_c} \quad (3)$$

3.4 Weight loss

The weight variations of the concrete specimens

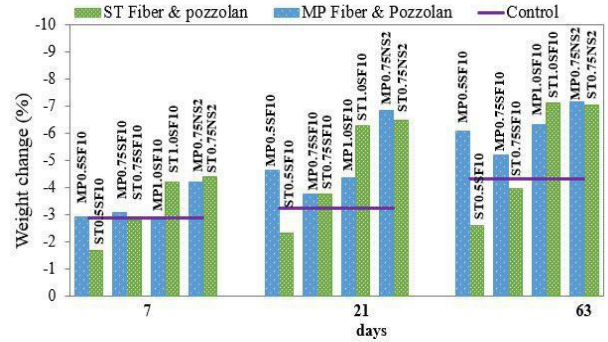


Fig. 20 Comparison between the weight loss of concrete specimens containing macro-polymeric fibers and those containing steel fibers versus immersion time in acid

containing macro-polymeric and steel fibers relative to the weight of the corresponding reference specimens (the specimens without exposure to acid) versus immersion time are given in Figs. 18 and 19, respectively, and their corresponding weights are given in Table 5. It is observed in the two figures that all the concrete specimens experience weight loss and erosion during the immersion time, with higher intensity at early immersion ages.

With respect to Fig. 18, it is found that by adding macro-polymeric fibers in the specimens containing silica fume, acid-induced weight loss decreases, indicating the inability of these fibers to resist against the erosion of high-strength concrete, in spite of the fact that previously, the bridging action of these fibers across matrix cracks was found to improve the compressive behavior of the specimens containing them against acid attack. Furthermore, resistance against erosion in the specimen containing macro-polymeric fibers at the volume fraction of 0.75% is greater compared with that of the other volume fractions (0.5 and 1.0%); a behavior previously observed for the crushing load and UPV. Weight loss after 63 days immersion in acid for the fiber-lacking concrete specimen and those containing 0.5, 0.75, and 1.0% macro-polymeric fibers compared to their weight after 28 days of curing without exposure to acid is 4.3, 6.1, 5.2, and 6.3%, respectively. Moreover, considering the results of the concrete containing 0.75% macro-polymeric fibers and 10% silica fume in comparison with those of the concrete containing 0.75% macro-polymeric fibers and 2% nano-silica, it can be concluded that the high replacement level of silica fume in the concrete relative to the low replacement level of nano-silica leads to lower weight loss for all the immersion days. This can be due to a lower potential of gypsum and ettringite production in the silica fume-containing specimen as a result of higher pozzolan content. The weight loss of the specimen containing 0.75% macro-polymeric fibers and 2% nano-silica is 7.2% after 63 days immersion, which represents the highest weight loss among all the specimens.

With respect to Fig. 19, it is found that by increasing the volume fraction of steel fibers up to 0.5% in the concrete specimens containing silica fume, a decrease in the trend of weight loss is resulted, while further increasing the content of steel fibers above that significantly increases the weight



Fig. 21 Surface texture of concrete specimens after 63 days immersion in 5% sulfuric acid solution

loss of the specimens relative to those without fibers.

However, the maximum values of the crushing load and UPV of the concrete specimens containing steel fibers and exposed to acid have previously occurred at the fiber volume fraction of 0.5%. The weight loss after 63 days immersion in sulfuric acid for the fiber-lacking concrete specimens and those containing 0.5, 0.75, and 1.0% steel fibers relative to that of the corresponding reference specimens is 4.3, 2.6, 4.0, and 7.1%, respectively. Moreover, by comparing the concrete containing 0.75% steel fibers and 10% silica fume with the one containing 0.75% steel fibers and 2% nano-silica (with 7.0% weight loss), it is seen that the effect of silica fume on the high-strength concrete durability during exposure to sulfuric acid attack is greater than that of nano-silica, due to the lower percentage of nano-silica used. The weight variations of the concrete specimens containing steel fibers relative to those of the specimens containing macro-polymeric fibers versus immersion time in sulfuric acid are plotted in Fig. 20, in which, as can be seen, the addition of both macro-polymeric and steel fibers to the concrete mix leads to the deterioration of erosion condition in comparison to the control (SF10) especially at high immersion ages. However, this is not the case for the specimens with low volume fractions of steel fibers, with the specimen containing 0.5% steel fibers (as the lowest fiber volume fraction) showing lower weight loss relative to the control. In addition, the weight loss of the concrete specimens containing steel fibers together with silica fume is greater compared with that of the specimens containing macro-polymeric fibers and silica fume at the highest fiber volume fraction ($V_f=1.0\%$). Note that using high volume fractions of fibers in high-strength concrete mixes leads to fiber agglomeration and the subsequent pore

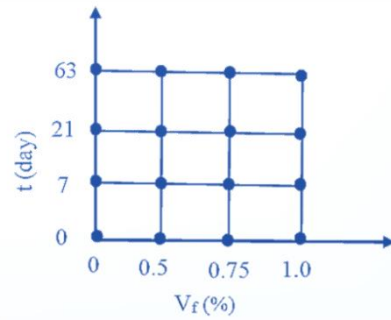


Fig. 22 Experimental design scheme for macro-polymeric and steel fibers

formation in the concrete; hence, acidic water can easily penetrate into the concrete and by washing calcium hydroxide to a high extent, the porosity and weight loss of concrete increase, thus the concrete becomes continuously weaker and more susceptible to acid attacks. It is also revealed from Fig. 20 that the weight loss values of the nano-silica-containing specimens, i.e., ST0.75NS2 and MP0.75NS2, are almost similar in all the immersion days.

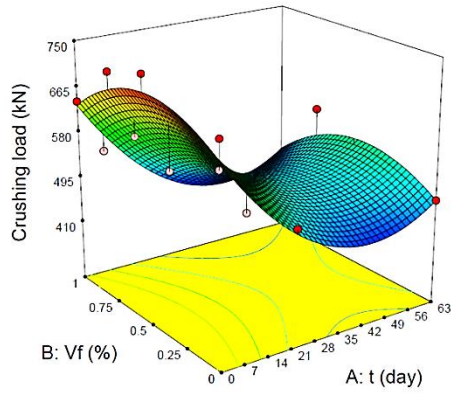
3.5 Visual inspection of specimens after exposure to acid

One important parameter regarding the structural members exposed to acid attack is the extent of corrosion in these members. In some cases, the corrosion is very severe and deep, and in some other, it is superficial and shallow. Therefore, the visual inspection of the specimens exposed to acid is of particular interest. The surface texture of the concrete specimens after 63 days immersion in the sulfuric acid solution is given in Fig. 21; with respect to which, in the concrete containing only silica fume (SF10), the ones with 0.5 and 1.0% macro-polymeric fibers, the one with 1.0% steel fibers, and the fibrous concretes containing nano-silica, after exposure to acid, the aggregates experience severe damage, and the cement mortar (surface mortar layer of concrete) is lost to a significant degree, indicating the higher vulnerability of these specimens to sulfuric acid attack. However, the surface of the specimens having 0.5 or 0.75% steel fibers together with 10% silica fume, as well as the one containing 0.75% macro-polymeric with 10% silica fume seem to have experienced a little change. This trend was predictable to a high degree considering the previously discussed weight loss and erosion condition of the concrete specimens.

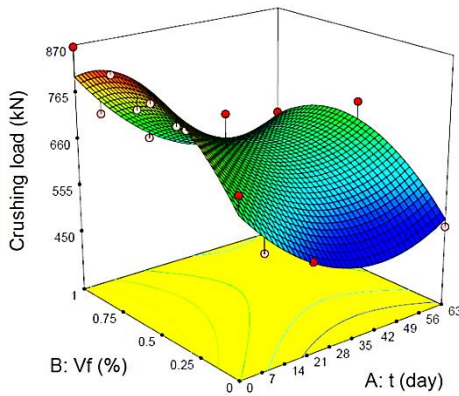
Concerning Fig. 21, it is found that the surface of the concrete specimens containing steel fibers experienced less erosion relative to that of the specimens containing macro-polymeric fibers, with the concrete containing 0.5% steel fibers and 10% silica fume (ST0.5SF10) possessing the best surface appearance among all the specimens, and except for some gypsum formed on the surface, it remained in general intact.

3.6 Optimization

Establishing a relationship between dependent and



(a) Macro-polymeric fibers



(b) Steel fibers

Fig. 23 Response surfaces corresponding to the models obtained from Eqs. (4) and (5)

independent variables is required in research and statistics. By developing a mathematical formulation between the dependent and independent variables, their variations as well as the maximum and minimum values can be easily predicted. Response surface method (RSM) and neural network method (NNM) are two of the most important data optimization and analysis methods which are applied in cases where the variables are more than one. Concerning the two mentioned methods, RSM has been favored over the other as a result of the simplicity it provides for obtaining response-associated equations in terms of several variables as well as the simplicity regarding presenting the data related to optimal conditions. In this work, the multi-objective simultaneous optimization technique was utilized using RSM as the basis for finding the best solution. In doing so, the commercially available program Design-Expert (2012) were used. The common response surface experimental plan used here to find response equations and determine optimal data values involves two variables, namely t and V_f , and four levels, namely $t=0, 7, 21, \text{ and } 63$; $V_f=0, 0.5, 0.75, \text{ and } 1.0\%$, and it is expressed in the form of full factorial experimental design for each fiber type. The general design scheme related to the number of given variables as well as the number of the levels of each variable for each fiber type is presented in Fig. 22. In this work, by employing the analysis of variance (ANOVA), 16 experimental data for each response (crushing load) of fibrous high-strength concrete were fitted to a mathematical

polynomial model. For macro-polymeric and steel fibers, the fitted regression models for the crushing load are written in the form of Eqs. (4) and (5), respectively,

For macro-polymeric fibers

$$P_c = 657.4 + 244.6V_f - 9.84t - 270.3V_f^2 + 0.11t^2 - 0.11V_f t \quad (4)$$

For steel fibers

$$P_c = 655.2 + 569.9V_f - 9.34t - 424.5V_f^2 + 0.11t^2 - 0.7V_f t \quad (5)$$

where V_f and t represent fiber volume fraction and immersion time, respectively. The coefficients of determination (R^2) for Eqs. (4) and (5) were obtained as 0.80 and 0.90, respectively. The response surfaces corresponding to the regression models obtained from the two above equations are presented in Fig. 23.

The numerical optimization method by using desirability functions (d_j) defined individually for each response (involving all the discussed variables and functions) can be applied to simultaneously optimize the responses (Derringer and Suich 1980, Köksal *et al.* 2013). Notice that all desirability functions (d_j) can only change in the range. The solution of a multi-objective optimization problem is conducted by using the single composite response (DR), which represents the geometric mean of individual desirability functions and is expressed by the following

$$DR = (d_1 \times d_2 \times d_3 \times \dots \times d_n)^{(1/n)} \quad (6)$$

where n is the number of responses of the optimization. Here, the feasible regions for conducting the optimization are

$$0\% \leq V_f \leq 1.0\% \quad (7)$$

$$0 \leq t \leq 63 \quad (8)$$

Obtaining a concrete that demonstrates the highest load-bearing capacity and the lowest weight loss while being under sulfuric acid attack is considered a significant accomplishment. Furthermore, to address cost-effectiveness concerns in the design of concrete, the cost of fibers (macro-polymeric and steel fibers) used in the making of composites also becomes influential. As a result, simultaneously maximizing the crushing load (P_c) and minimizing weight loss as well as V_f is necessary. For $n=3$, Eq. (6) can be rewritten as

$$DR = (d_1 \times d_2 \times d_3)^{(1/3)} \quad (9)$$

where d_1 , d_2 , and d_3 are the desirability functions of P_c , weight loss, and V_f , respectively. Tables 6 and 7 present the optimization solution for concretes having macro-polymeric or steel fibers, respectively. With respect to the tables, the optimum values of the volume contents of macro-polymeric and steel fibers in the concrete containing silica fume, when the crushing load is maximized and weight loss is minimized, are 0.06 and 0.34%, respectively.

Table 6 Optimum solution for concrete containing macro-polymeric fibers, when P_c is maximized and weight loss and V_f are minimized

	Target	Limits		Optimum solutions for 63 days
		Lower	Upper	
t , day	0; 7; 21; 63	0	63	63
Fiber volume fraction (V_f), %	Minimum	0	1.0	0.06
Crushing load (P_c), kN	Maximum	420	743.5	504.1
Weight loss, %	Minimum	0	6.33	4.51

Table 7 Optimum solution for concrete containing steel fibers, when P_c is maximized and weight loss and V_f are minimized

	Target	Limits		Optimum solutions for 63 days
		Lower	Upper	
t , day	0; 7; 21; 63	0	63	63
Fiber volume fraction (V_f), %	Minimum	0	1.0	0.34
Crushing load (P_c), kN	Maximum	491.7	866.0	638.2
Weight loss, %	Minimum	0	7.12	2.95

4. Conclusions

In the present work, the effect of sulfuric acid attack on the resistance and durability of high-strength concrete containing different percentages of macro-polymeric or steel fibers in the presence of silica fume and nano-silica pozzolans was investigated, and the experimental results including the crushing load, weight loss, ultrasonic pulse velocity (UPV), and surface appearance, were determined and subsequently evaluated. Furthermore, an optimum solution for the design parameters, for which the crushing load of fiber-reinforced concrete is maximized, was found using response surface method (RSM). Based on the results obtained here, the following conclusions can be drawn:

- The crushing load reduction of the concrete specimens containing macro-polymeric or steel fibers together with silica fume is more intense at early immersion ages in acid solution; however, after 21 days immersion, their strength reduction rate shows decreases considerably. The lowest crushing load reduction in the concrete containing macro-polymeric or steel fibers belongs to MP0.75SF10 and ST0.5SF10 (with 20.8 and 12.5% reduction, respectively).
- The use of 10% silica fume in comparison with 2% nano-silica as a cement-replacement in the specimen containing 0.75% steel fibers and the one with 0.75% macro-polymeric fibers leads to a decrease in the reduction of crushing load, UPV, and weight, as well as an increase in the durability of high-strength concrete against sulfuric acid attack. Furthermore, fibrous concretes containing nano-silica (ST0.75NS2 or MP0.75NS2) show the highest reduction of strength, UPV, and weight among all the specimens.
- Compared to macro-polymeric fibers, steel fibers leads

to lower UPV loss under acid attack for all the fiber volume fractions in the concrete specimens containing silica fume. Moreover, at a high volume fraction of fibers, the crushing load loss difference between the concretes containing steel fibers and those with macro-polymeric fibers decreases, while the weight loss of the specimens containing steel fibers is greater relative to that of the specimens containing macro-polymeric fibers.

- The crushing load and UPV of the fibrous concrete specimens have almost similar decreasing trends against immersion time. However, the UPV reduction percentage is lower compared with that of crushing load. Furthermore, a good similarity exists between the variations of these two parameters against the volume fraction of macro-polymeric and steel fibers, with the best performance against sulfuric acid attack having been achieved by adding 0.5% steel fibers or 0.75% macro-polymeric fibers in the concrete specimens containing these two fibers types.
- A general relationship between the crushing load and UPV with an exponential form was proposed for all the results of high-strength concrete specimens containing various pozzolans, fibers, and fiber volume fractions when exposed to sulfuric acid at different immersion ages, and the corresponding results show a good correlation with the experimental results.
- Erosion resistance in the specimens containing macro-polymeric fibers at the volume fraction of 0.75% is greater relative to that of the other volume fractions (0.5 and 1.0%); a behavior similar to the one previously observed for crushing load and UPV. In addition, as the volume fraction of steel fibers increases up to 0.5%, the weight loss of concrete specimens decreases, while its further increase above that threshold considerably increases the weight loss of the specimens.
- The visual inspection of the specimens' surface showed that the fiber-lacking concrete containing silica fume, the ones containing 0.5 or 1.0% macro-polymeric fibers, and the one with 1.0% steel fibers, as well as the fibrous concretes containing nano-silica suffered significant damage after exposure to the sulfuric acid solution, while the concrete specimens having lower weight losses (ST0.5SF10, ST0.75SF10, and MP0.75SF10) suffered only a little damage. Furthermore, the surface of the specimens reinforced with steel fibers experienced less erosion relative to that of the specimens reinforced with macro-polymeric fibers.
- The optimum volume fraction of macro-polymeric and steel fibers in the concrete containing silica fume, for which the crushing load values are maximized and the weight loss values are minimized was obtained as 0.06 and 0.34%, respectively.

References

- ACI Committee 211 (2008), Guide for Selecting Proportions for High-Strength Concrete Using Portland Cement and Other Cementitious Materials ACI 211.4R-08, American Concrete

- Institute, Farmington Hills (MI).
- Afroughsabet, V. and Ozbakkaloglu, T. (2015), "Mechanical and durability properties of high-strength concrete containing steel and polypropylene fibers", *Constr. Build. Mater.*, **94**, 73-82.
- Araghi, H.J., Nikbin, I.M., Reskati, S.R., Rahmani, E. and Allahyari, H. (2015), "An experimental investigation on the erosion resistance of concrete containing various PET particles percentages against sulfuric acid attack", *Constr. Build. Mater.*, **77**, 461-471.
- Aslani, F. and Natoori, M. (2013), "Stress-strain relationships for steel fibre reinforced self-compacting concrete", *Struct. Eng. Mech.*, **46**(2), 295-322.
- ASTM C143/C143M (2015), "Standard Test Method for Slump of Hydraulic-Cement Concrete", American Society for Testing and Materials International, United States.
- ASTM C597 (2016), "Standard test method for pulse velocity through concrete", United States: American Society for Testing and Materials International.
- Bogas, J.A., Gomes, M.G. and Gomes, A. (2013), "Compressive strength evaluation of structural lightweight concrete by non-destructive ultrasonic pulse velocity method", *Ultrasonics*, **53**(5), 962-972.
- BS 1881-116 (1983), Testing Concretes, Method for determination of compressive strength of concrete cubes.
- Chang, Z.T., Song, X.J., Munn, R. and Marosszeky, M. (2005), "Using limestone aggregates and different cements for enhancing resistance of concrete to sulphuric acid attack", *Cement Concrete Res.*, **35**(8), 1486-1494.
- Derringer, G. and Suich, R. (1980), "Simultaneous optimization of several response variables", *J. Qual. Technol.*, **12**(4), 214-219.
- Design-Expert (R) 8 software (2012), Stat-Ease, Inc., Minneapolis, MN, USA 2012.
- Ehrich, S., Helard, L., Letourneux, R., Willocq, J. and Bock, E. (1999), "Biogenic and chemical sulfuric acid corrosion of mortars", *J. Mater. Civil Eng.*, **11**(4), 340-344.
- Fallah, S. and Nematzadeh, M. (2017), "Mechanical properties and durability of high-strength concrete containing macro-polymeric and polypropylene fibers with nano-silica and silica fume", *Constr. Build. Mater.*, **132**, 170-187.
- Fattuhi, N.I. and Hughes, B.P. (1988), "Ordinary Portland cement mixes with selected admixtures subjected to sulfuric acid attack", *Mater. J.*, **85**(6), 512-518.
- Hasan-Nattaj, F. and Nematzadeh, M. (2017), "The effect of fortaferro and steel fibers on mechanical properties of high-strength concrete with and without silica fume and nano-silica", *Constr. Build. Mater.*, **137**, 557-572.
- Hernández, M.G., Izquierdo, M.A.G., Ibáñez, A., Anaya, J.J. and Ullate, L.G. (2000), "Porosity estimation of concrete by ultrasonic NDE", *Ultrasonics*, **38**(1), 531-533.
- Hobbs, D.W. and Taylor, M.G. (2000), "Nature of the thaumasite sulfate attack mechanism in field concrete", *Cement Concrete Res.*, **30**(4), 529-533.
- Hsu, L.S. and Hsu, C.T. (1994), "Stress-strain behavior of steel-fiber high-strength concrete under compression", *Struct. J.*, **91**(4), 448-457.
- Hwang, J.P., Jung, M.S., Kim, M. and Ann, K.Y. (2015), "Corrosion risk of steel fibre in concrete", *Constr. Build. Mater.*, **101**, 239-245.
- Kim, B., Boyd, A.J., Kim, H.S. and Lee, S.H. (2015), "Steel and synthetic types of fiber reinforced concrete exposed to chemical erosion", *Constr. Build. Mater.*, **93**, 720-728.
- Köksal, F., Şahin, Y., Gencel, O. and Yiğit, İ. (2013), "Fracture energy-based optimisation of steel fibre reinforced concretes", *Eng. Fract. Mech.*, **107**, 29-37.
- Lee, S.T., Hooton, R.D., Jung, H.S., Park, D.H. and Choi, C.S. (2008), "Effect of limestone filler on the deterioration of mortars and pastes exposed to sulfate solutions at ambient temperature", *Cement Concrete Res.*, **38**(1), 68-76.
- Mangat, P.S. and Gurusamy, K. (1988), "Corrosion resistance of steel fibres in concrete under marine exposure", *Cement Concrete Res.*, **8**(1), 44-54.
- Mehta, P.K. (1985), "Studies on chemical resistance of low water/cement ratio concretes", *Cement Concrete Res.*, **15**(6), 969-978.
- Miao, C., Mu, R., Tian, Q. and Sun, W. (2002), "Effect of sulfate solution on the frost resistance of concrete with and without steel fiber reinforcement", *Cement Concrete Res.*, **32**(1), 31-34.
- Monteny, J., De Belie, N., Vincke, E., Verstraete, W. and Taerwe, L. (2001), "Chemical and microbiological tests to simulate sulfuric acid corrosion of polymer-modified concrete", *Cement Concrete Res.*, **31**(9), 1359-1365.
- Monteny, J., Vincke, E., Beeldens, A., De Belie, N., Taerwe, L., Van Gemert, D. and Verstraete, W. (2000), "Chemical, microbiological, and in situ test methods for biogenic sulfuric acid corrosion of concrete", *Cement Concrete Res.*, **30**(4), 623-634.
- Naffa, S.O., Goueygou, M., Piwakowski, B. and Buyle-Bodin, F. (2002), "Detection of chemical damage in concrete using ultrasound", *Ultrasonics*, **40**(1), 247-251.
- Nematzadeh M. and Hasan-Nattaj, F. (2017), "Compressive stress-strain model for high-strength concrete reinforced with fortaferro and steel fibers", *J. Mater. Civil Eng.*, **29**(10), 04017152.
- Nwokoye, D.N. and Eng, C. (1974), "Assessment of the elastic moduli of cement paste and mortar phases in concrete from pulse velocity tests", *Cement Concrete Res.*, **4**(4), 641-655.
- Rahimi, S., Nikbin, I.M., Allahyari, H. and Habibi, S. (2016), "Sustainable approach for recycling waste tire rubber and polyethylene terephthalate (PET) to produce green concrete with resistance against sulfuric acid attack", *J. Clean. Product.*, **126**, 166-177.
- Santhanam, M., Cohen, M.D. and Olek, J. (2002), "Mechanism of sulfate attack: A fresh look: Part 1: Summary of experimental results", *Cement Concrete Res.*, **32**(6), 915-921.
- Schmidt, T., Lothenbach, B., Romer, M., Neuenchwander, J. and Scrivener, K. (2009), "Physical and microstructural aspects of sulfate attack on ordinary and limestone blended Portland cements", *Cement Concrete Res.*, **39**(12), 1111-1121.
- Shannag, M.J. (2000), "High strength concrete containing natural pozzolan and silica fume", *Cement Concrete Compos.*, **22**(6), 399-406.
- Solis-Carcaño, R. and Moreno, E.I. (2008), "Evaluation of concrete made with crushed limestone aggregate based on ultrasonic pulse velocity", *Constr. Build. Mater.*, **22**(6), 1225-1231.
- Suleiman, A.R., Soliman, A.M. and Nehdi, M.L. (2014), "Effect of surface treatment on durability of concrete exposed to physical sulfate attack", *Constr. Build. Mater.*, **73**, 674-681.
- Tamimi, A.K. (1997), "High-performance concrete mix for an optimum protection in acidic conditions", *Mater. Struct.*, **30**(3), 188-191.
- Torii, K. and Kawamura, M. (1994), "Effects of fly ash and silica fume on the resistance of mortar to sulfuric acid and sulfate attack", *Cement Concrete Res.*, **24**(2), 361-370.
- Trtnik, G., Kavčič, F. and Turk, G. (2009), "Prediction of concrete strength using ultrasonic pulse velocity and artificial neural networks", *Ultrasonics*, **49**(1), 53-60.
- Zarrin, O. and Khoshnoud, H.R. (2016), "Experimental investigation on self-compacting concrete reinforced with steel fibers", *Struct. Eng. Mech.*, **59**(1), 133-151.